we used AR2H mice at 14 weeks and 17 weeks of age as representatives of presymptomatic stage mice, AR2 at 15 weeks of age and AR2H mice at 74 weeks as representatives of early symptomatic stage mice, and AR2Slow mice at 140 weeks of age as representatives of late symptomatic stage mice. We also examined the AR2res mice at 28 weeks and 58 weeks of age to examine the role of exaggerated Ca^{2+} influx through the AMPA receptors in the formation of nuclear vacuoles.

2.1. *Presymptomatic stage mice (AR2H mice, 14 weeks and 17 weeks)*

Light-microscopically, anterior horn neurons were relatively well-preserved, but some large anterior horn neurons showed simple atrophy by H&E staining, exhibiting a dark, basophilic, and shrunken appearance. On the plastic sections stained with toluidine blue of the cervical spinal cord of AR2H mice, some large motor neurons with simple atrophy were scattered in the anterior horn, accompanied by astrogliosis. Anterior and posterior horn neurons showed no vacuoles in the cytoplasm or nucleus. There were no myelin ovoids in the white matter, anterior roots or posterior roots.

Electron-microscopically, most of the anterior horn neurons were normal-appearing, but some showed simple atrophy with small vacuoles in the cytoplasm. The cisterns of endoplasmic reticulum (ER) were well-preserved in the cytoplasm of normal-appearing motor neurons, except for slight dilatation. Mitochondria were almost always normal-looking, showing no vacuoles or electron-dense changes of the inner and outer membranes and cristae.

These light- and electron-microscopic changes were similar to those observed in age-matched wild type mice.

2.2. *Early symptomatic stage mice (AR2 mice, 15 weeks, AR2H mice, 74 weeks)*

Light-microscopically, in AR2 mice at 15 weeks of age, anterior horn neurons of the cervical spinal cord were relatively well-preserved, but some large anterior horn neurons showed simple atrophy by H&E staining, exhibiting a dark, basophilic, and shrunken appearance. On the plastic sections stained with toluidine blue, some large motor neurons with simple atrophy were scattered in the anterior horn, accompanied by astrogliosis. Anterior and posterior horn neurons showed no vacuoles in the cytoplasm or nucleus. There were no myelin ovoids in the white matter, anterior roots or posterior roots. In AR2H mice at 74 weeks of age, the motor neurons of the cervical spinal cord were definitely reduced in number, and there were numerous degenerating anterior horn neurons with nuclear vacuolization by H&E staining (Fig. 2(a) and (b)). On the plastic sections stained with toluidine blue, most of the motor neurons, except a few large ones which were well-preserved, showed various sizes of vacuoles in the cytoplasm or nuclei. This was the case for both of the anterior horn neurons (Fig. 3(a) and (b)), and to a lesser extent of the posterior horn neurons. Vacuolation was observed predominantly within the nuclei of motor neurons, and less frequently in the somata. Myelin ovoids and swellings of myelin sheaths were frequently found in the anterior column and anterior roots, and to a lesser extent in the lateral and posterior columns and posterior roots.

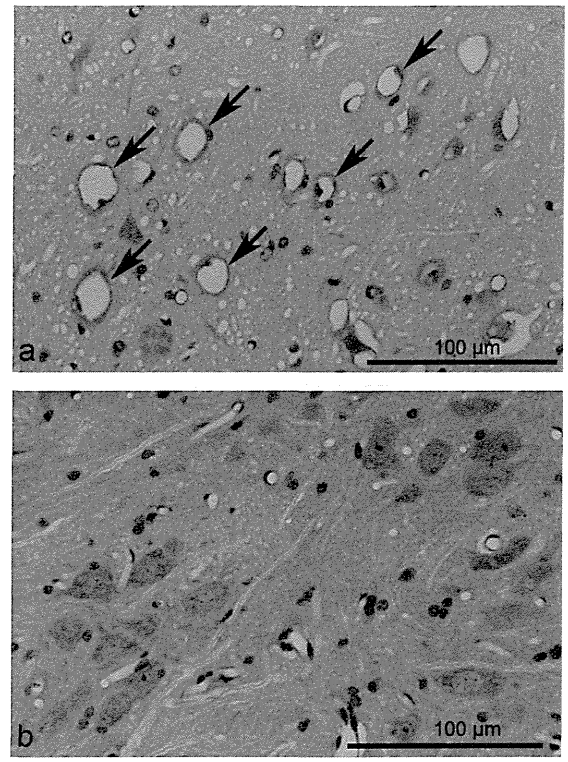

Fig. 2 – Light micrograph of an anterior horn neuron. (a) Anterior horn neurons show degenerative change with vacuolation (arrows), (AR2H mouse, 74 weeks, early symptomatic stage). H&E staining. (b) Normal anterior horn neurons for comparison (Control mouse, 74 weeks). H&E staining.

Electron-microscopically, in AR2 mice, a few of the large anterior horn neurons showed simple atrophy, but most of them exhibited normal-looking cytoplasm containing abundant rough ER, mitochondria, lipofuscin granules and lysosomes. Small vacuoles were occasionally exhibited in the cytoplasm of motor neurons, most of which were non-membrane-bound (Fig. 4(a) and (b)). While the cytoplasm of motor neurons was relatively well-preserved, the interior of dendrites was frequently loose and disorganized, containing electron-dense membranous structures. Mitochondria did not exhibit any prominent vacuolar change. Astrocytes and oligodendrocytes did not show vacuolation in the cytoplasm or nucleus, although the lumen of ER in glial cells was frequently dilated. In AR2H mice, single or multiple vacuolar changes without a limiting membrane were frequently observed in the nuclei, and to a lesser extent in the somata and dendrites, of the anterior horn neurons. Vacuolation was less frequently observed in the nuclei and the somata of posterior horn neurons than in that of anterior horn neurons. Vacuolar changes were also often seen in the nuclei of astrocytes (Fig. 5(a) and (b)) and oligodendrocytes (Fig. 5(c) and (d)) in the anterior horns, and to a lesser extent in the posterior horns. The vacuoles were varied in size, with some

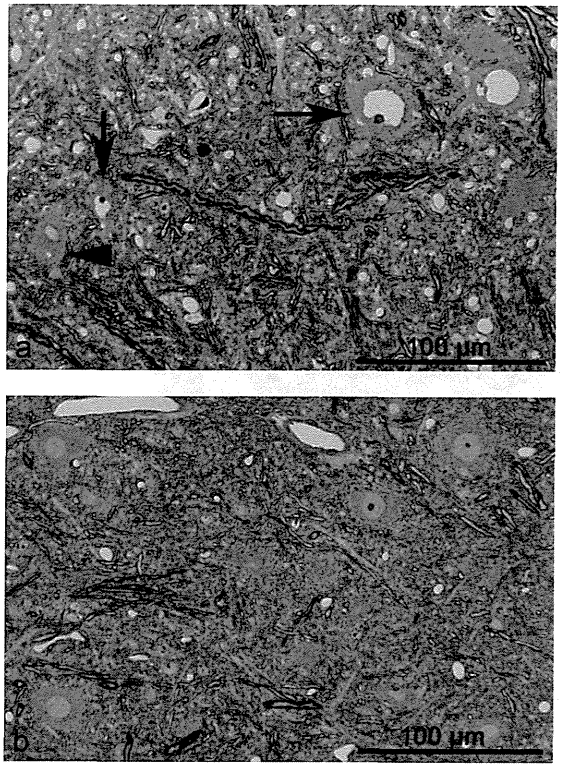

Fig. 3 – Semi-thin section of an anterior horn stained with toluidine blue. (a) Most anterior horn neurons show vacuoles of various sizes in the cytoplasm (arrow head) and nuclei (arrows) (AR2H mouse, 74 weeks). (b) Anterior horn neurons are well-preserved, and show no vacuoles in the cytoplasm or nucleus (Control mouse, 74 weeks).

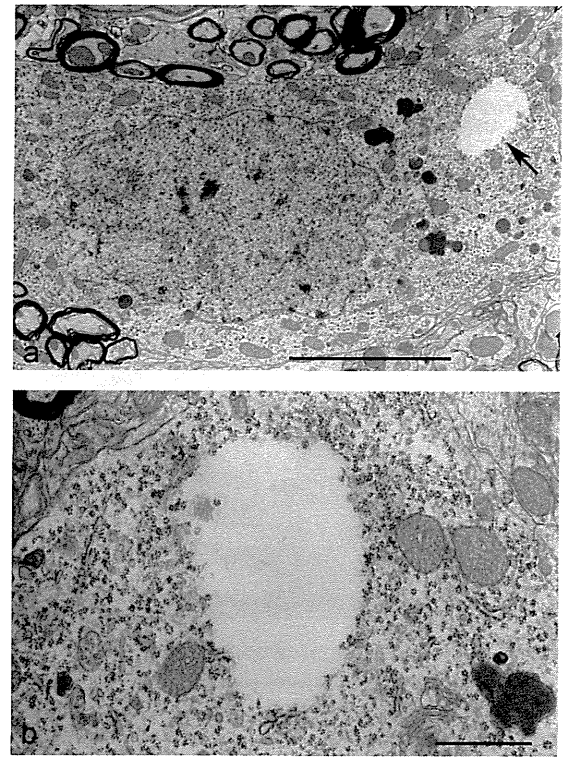

Fig. 4 – Electron micrograph of small vacuolation in the cytoplasm of AR2 mouse. (a) A microvacuolation (arrow) observed in the cytoplasm of a large motor neuron (AR2 mouse, 15 weeks). Scale bar: 1 μm. (b) A higher magnification of Fig. 4(a). The vacuole has neither limiting membrane nor organelle. Scale bar: 1 μm.

being large enough to occupy the whole nucleus, and they occasionally contained membranous structures within them (Fig. 5(a) and (c)). Mitochondria and the cisterns of ER in the cytoplasm of motor neurons, oligodendrocytes and astrocytes were relatively well-preserved. However, the lumen of the rough ER was occasionally dilated with splitting of the membrane of the cisternae, expanding into vacuoles.

2.3. *Late symptomatic stage mice (AR2Slow mice, 140 weeks)*

Light-microscopically, the motor neurons were definitely reduced in number, and there were numerous degenerating anterior horn neurons with nuclear vacuolization by H&E staining. On the plastic sections stained with toluidine blue, the pathology of the spinal cord was very similar to that of AR2H mice (74 weeks): some large motor neurons were well-preserved, but the majority of neurons showed vacuolar changes in anterior horn neurons, and less conspicuously in the posterior horn neurons. In addition, myelin ovoids and swellings of the myelin sheaths were prominent in the anterior and posterior columns and in anterior roots, and to a lesser extent in the lateral column and posterior roots.

Electron-microscopically, the pathological changes were similar to those observed in AR2H mice (74 weeks). Vacuolar changes were preferentially observed in the nuclei of motor neurons, frequently spreading over the whole nuclei, and to a lesser extent in the somata and dendrites. The nuclei of motor neurons exhibited a few small vacuoles (Fig. 6(a)) or a large vacuole occupying almost the whole nucleus with no vacuoles in the cytoplasm (Fig. 6(b), (c) and (d)). A few vacuoles were also observed in the cytoplasm without any vacuole in the nuclei. Although most of the cisternae of ER were well-preserved, the lumen of the rough ER in the cytoplasm of motor neurons was occasionally dilated with splitting of the membrane of the cisternae, expanding into vacuoles. In addition, there were some small vacuoles originating in the Golgi apparatus. Vacuolation was also observed less frequently in the nuclei of posterior horn neurons than in those of anterior horn neurons, and to a limited extent in the somata. Astrocytes and oligodendrocytes in the anterior horn also showed frequent vacuolation in the nuclei, containing a membranous substance without vacuolar change in the cytoplasm. Those in the posterior horn to a lesser extent showed similar characteristics. The somata and dendrites of anterior horn neurons often contained electron-dense membranous structures. Mitochondria in the cytoplasm of motor neurons, oligodendrocytes and astrocytes were well-preserved. The anterior roots were often degenerated, showing shrunken and atrophic axons enclosed by a collapsed and folded myelin sheath. Light-and electron-microscopically,

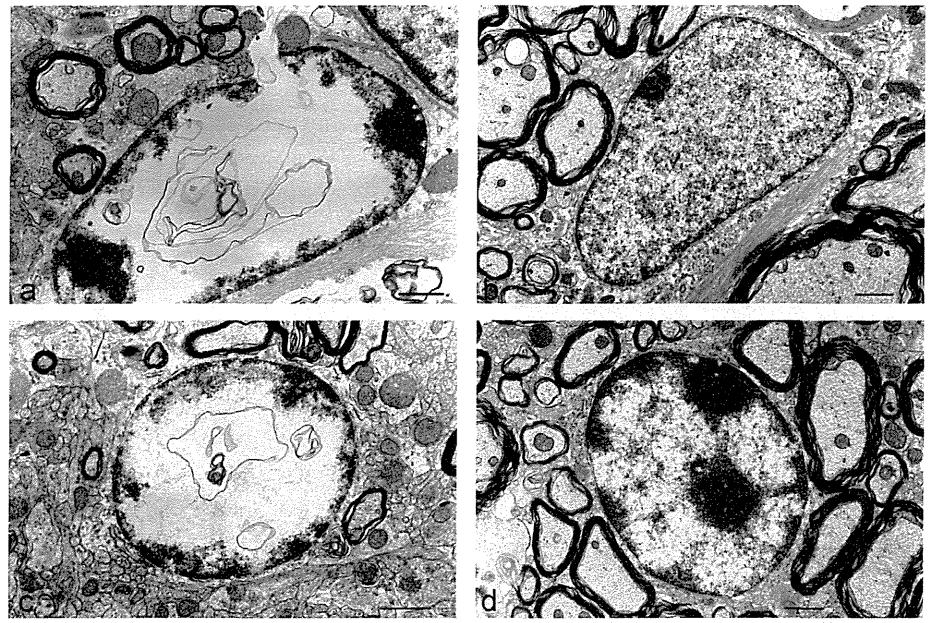

Fig. 5 – Electron micrographs of nuclear vacuolation in glial cells. (a) The nucleus of an astrocyte shows vacuolar change and includes membranous structures (AR2H mouse, 74 weeks). Scale bar: 1 μm. (b) An astrocyte of a control shown for comparison (20 weeks). Scale bar: 1 μm. (c) The nucleus of an oligodendrocyte shows vacuolar change and includes membranous structures (AR2H mouse, 74 weeks). Scale bar: 1 μm. (d) An oligodendrocyte of a control shown for comparison (20 weeks). Scale bar: 1 μm.

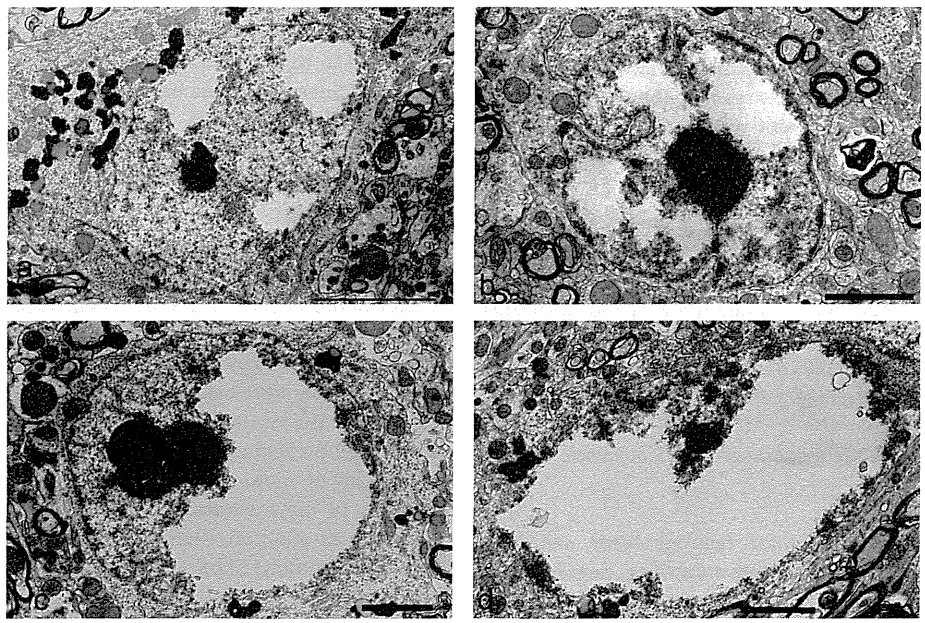

Fig. 6 – Electron micrographs of nuclear vacuolation in a motor neuron (AR2Slow mouse, 140 weeks). (a) The nucleus of a motor neuron exhibits three small vacuoles in the interior. Scale bar: 1 μm. (b) There are cytoplasmic intrusions into the nucleus of a motor neuron. The nucleus contains multiple vacuoles. Scale bar: 0.5 μm. (c) The nucleus of a motor neuron is distended by a relatively large nuclear vacuole that seems to push chromatin. Scale bar: 0.5 μm. (d) Almost all of the nucleoplasm is distended by a large vacuole that appears to push chromatin and nucleolus up against the nuclear membrane. The nuclear membrane is partly obscure. Scale bar: 0.5 μm.

anterior horn neurons appeared well-preserved in age-matched wild type control mice, although some large anterior horn neurons showed simple atrophy (Fig. 7).

The major light- and electron-microscopic findings for each experimental group from presymptomatic to late symptomatic stages are summarized in Table 1.

2.4. AR2res mice (28 weeks and 58 weeks)

ADAR2flox alleles are targeted by Cre in the same time course as are AR2 mice, but endogenous GluA2 gene are engineered to express Q/R site-edited GluA2 in AR2res mice. Therefore ADAR2-lacking motor neurons express Ca^{2+}-impermeable AMPA receptors that contain Q/R site-edited GluA2 as motor neurons of wild-type and AR2res mice exhibit normal behavior without loss of motor neurons (Hideyama et al., 2010). There were no nuclear vacuoles in the anterior horn neurons of AR2res mice (28 weeks and 58 weeks), or age-matched wild-type mice (12 weeks, 14 weeks, 15 weeks, 16 weeks, 17 weeks, 28 weeks, 74 weeks and 135 weeks).

2.5. Quantitative data on nuclear vacuoles in motor neurons

To examine whether the formation of nuclear vacuoles results from ADAR2 downregulation, we examined the number of large motor neurons bearing nuclear vacuoles in AR2H mice at different ages. In all the AR2H mice (and AR2 mice, not shown) irrespective of the age examined, there were large motor neurons in the spinal cord exhibiting vacuoles in their nuclei (Fig. 8). Motor neurons with nuclear vacuoles were most frequent at 2 months of age but were observed even in mice over 2 years of age. The number of vacuole-bearing anterior horn neurons decreased with the loss of anterior horn neurons after 40 weeks of age in AR2H mice (Fig. 8). We could not observe nuclear vacuoles in motor neurons of wild-type mice at the comparable ages.

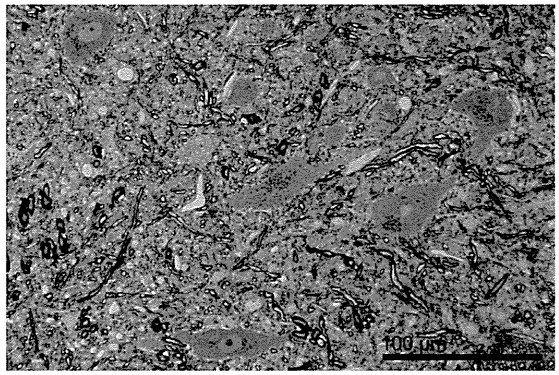

Fig. 7 – Normal anterior horn neurons for comparison (Age-matched wild type mouse, 135 weeks).

2.6. Postmortem analysis

Because nuclear vacuoles such as those presented here have not been reported in neurons or other cells in the central nervous system, including motor neurons of patients with ALS, we examined the effects of postmortem delay on the nuclear vacuole. All the AR2 mice (34 weeks, 30 weeks and 34 weeks) examined at 1 h, 6 h and 24 h, respectively after death showed no nuclear vacuoles of motor neurons.

3. Discussion

Many pathogenic mechanisms have been proposed as possible causes of motor neuron degeneration in ALS. Neuronal excitotoxicity from excessive extracellular glutamate is one of the potential candidates for the pathogenesis of ALS (Rothstein et al., 1992; Rothstein et al., 1995). In connection with the neuronal excitotoxicity, inefficient GluA2 Q/R site-RNA editing found in motor neurons may be associated with the pathogenesis of sporadic ALS (Kawahara et al., 2004; Kwak and Kawahara, 2005). That is, unedited GluA2 mRNA at the Q/R site and the decreased level of ADAR2 mRNA are expressed specifically in sporadic ALS patients and selectively in their motor neurons (Kawahara et al., 2004; Kawahara et al., 2006; Akbarian et al., 1995; Hideyama et al., 2012a). The neuronal loss of ADAR2-lacking anterior horn neurons in AR2

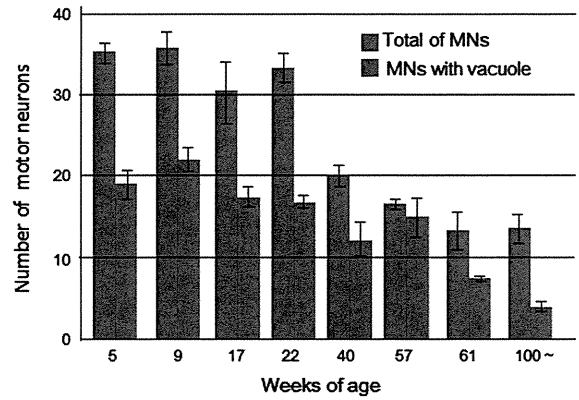

Fig. 8 – Quantitative data on nuclear vacuoles in motor neurons of the AR2H mice. The total number of anterior horn neurons at each age in AR2H mice is shown (mean ± SEM). The number of vacuole-bearing anterior horn neurons (mean ± SEM) decreased with the loss of anterior horn neurons after 40 weeks of age in AR2H mice. (n=3–4).

Table 1 – Summary of the pathological changes in conditional ADAR2-knockout mice.

	Light-microscopic findings		Electron-microscopic findings
	Nuclear vacuoles (motor neurons)	White matter changes (myelin ovoids)	Nuclear vacuoles (neurons and glia)
Presymptomatic AR2H (14 and 17 weeks)	Absent	Absent	Absent
Early symptomatic AR2 (15 weeks)	Absent	Absent	Absent
Early symptomatic AR2H (74 weeks)	Present	Present	Present
Late symptomatic AR2Slow (140 weeks)	Present	Present	Present

mice was completely prevented in AR2res mice, in which the endogenous GluA2 alleles are engineered to express the R codon (CGG) instead of Q codon (CAG) at the Q/R site, thus enabling ADAR2-lacking motor neurons to express Q/R site-edited GluA2 in the absence of ADAR2 (Hideyama et al., 2010). These findings indicate the crucial role of RNA editing at the GluA2 Q/R site for the survival of motor neurons and demonstrate that expression of Q/R site-unedited GluA2 is a cause of the slow death of motor neurons.

The results obtained from AR2 mice indicate that motor neurons undergo Ca^{2+}-permeable AMPA receptor-mediated slow death (Hideyama et al., 2010). In addition, AR2 mice possess certain characteristics found in sporadic ALS, including slow progressive death of motor neurons, neuromuscular unit-dependent motor dysfunction, the selective vulnerability of facial and hypoglossal nerve nuclei, and differential low vulnerability of the motor neurons of extraocular muscles, even though the extent of GluA2 Q/R site editing is significantly reduced in the oculomotor nerve nuclei (Hideyama et al., 2010). Moreover, motor neurons of AR2 and AR2H mice exhibit mislocalization of TDP-43, a pathological hallmark of ALS, via activation of calcium-dependent protease calpain (Yamashita et al., 2012). Expression of unedited GluA2-containing Ca^{2+}-permeable AMPA receptors results in activation of calpain-dependent cleavage of TDP-43 into aggregation-prone fragments in the motor neurons of AR2 mice, suggesting a molecular mechanism underlying TDP-43 pathology in ALS motor neurons. Thus, conditional ADAR2-knockout mice are considered to be a more specific animal model for sporadic ALS.

In the previous study of AR2 mice (early symptomatic stage), we reported several degenerating large motor neurons with cytoplasmic vacuoles and a significantly decreased number of ADAR2-lacking motor neurons between 1 and 2 months of age, while the number of ADAR2-positive motor neurons remained unchanged after 2 months of age (Hideyama et al., 2010). In this study, some novel findings were found preferentially in the anterior horns in homozygous and heterozygous ADAR2-knockout mice, related to the pathomechanism of motor neuron degeneration.

First, vacuolation in the nuclei of anterior horn neurons was the most conspicuous finding. Cytoplasmic vacuolation of motor neurons is fairly common after a variety of insults, such as tetanus (Müller and Jeschke, 1971) and type C viral infection (Andrews and Andrews, 1976), as well as in the mutant wobbler mouse (Andrews and Andrews, 1976; Andrews and Maxwell, 1969) and SOD1-related animal models for ALS (Dal Canto and Gurney, 1995; Sasaki et al., 2004), but is quite rare in human motor neuron diseases (Chou, 1979; Hirano and Iwata, 1979; Kohn, 1971; Reif-Kohn and Munde, 1974; Sasaki et al., 1998). In particular, there have been no reports of the presence of nuclear vacuoles in sporadic ALS patients, except for the presence of vacuoles in the cytoplasm of motor neurons. With respect to the origin of the vacuolization, in mice possessing the G93A and G37 mutant SOD1, vacuolar changes are derived from the inner compartment and the intermembrane space of mitochondria with splitting of the outer and inner membranes (Dal Canto and Gurney, 1995; Sasaki et al., 2004). Moreover, in experimental type C viral infection and the wobbler mouse, the vacuolation results from destruction of the ER (Andrews and Andrews, 1976; Andrews and Maxwell, 1969). Thus, in all of the previously reported cases, the vacuolation exclusively occurs in the somata of motor neurons, but not in the nuclei. Because nuclear vacuoles were observed in some motor neurons of all AR2 and AR2H mice examined, this unique morphological change is likely closely associated with the increase of Ca^{2+} influx through the unedited GluA2-containing AMPA receptors and is relevant to the death of motor neurons. The proportion of anterior horn neurons with nuclear vacuoles was highest at 0.5 years of age. When the active degeneration of ADAR2-lacking anterior horn neurons underwent active microglial proliferation (Hideyama et al., 2010), indicating that the presence of nuclear vacuole is closely related to the neuronal death. The decrease in the number of anterior horn neurons with nuclear vacuoles after 0.5 years of age may represent the decline of degenerating anterior horn neurons with age (Hideyama et al., 2010). The bidirectional trafficking of molecules between the cytoplasm and the nucleus is performed through the nuclear pore complex in the nuclear envelope using nucleo-cytoplasmic transport. Changes in cytosolic Ca^{2+} can promote translocation of transcription factors or transcriptional regulators from the cytosol to the nucleus, whereas changes in nucleoplasmic Ca^{2+} can also directly regulate gene expression (Alonso and García-Sancho, 2011). Recently, there has been increasing evidence indicating that both passive and facilitated nucleo-cytoplasmic transport of small molecules and larger molecules, respectively, can be regulated by Ca^{2+} stores in the perinuclear spaces of the nuclear envelope and the cisternal spaces of the endoplasmic reticulum (Corbett and Silver, 1997; Miao and Schulten, 2009). Moreover, the malfunction of nucleo-cytoplasmic transport caused by changes in Ca^{2+} is associated with degenerative diseases (Mattson et al., 2000). Notably, there were no nuclear vacuoles in the anterior horn neurons of AR2res mice or in age-matched wild-type mice in this study. In AR2res mice, the endogenous GluA2 gene is engineered to express Q/R site-edited GluA2, rendering these mice to express normal Ca^{2+}-impermeable AMPA receptors in the absence of ADAR2. Thus, vacuoles in the nuclei of motor neurons in our mutant mice result from the increased cytosolic Ca^{2+} through Ca^{2+}-permeable AMPA receptors with resultant changes in nucleoplasmic Ca^{2+} through the malfunction of nucleo-cytoplasmic transport, rather than the failure of RNA editing at ADAR2-mediated positions other than the GluA2 Q/R site. It is predictable that large nuclear vacuoles in some surviving motor neurons in the aged mice may be a consequence of continued Ca^{2+}-mediated nuclear vacuole formation under the condition of elevated Ca^{2+} concentration. Age-related ADAR2 downregulation may participate in the chronic rise of Ca^{2+} concentration in the motor neurons of aged mice (Hideyama et al., 2012b). On the other hand, with regard to the origin of vacuoles in the cytoplasm of motor neurons in this model mouse, a dilatation of the ER may contribute to the vacuolization, judging from the largely dilated lumen of the ER with splitting of the membrane of the cisternae. The changes in the ER may elicit a Ca^{2+} load imbalance in the ER lumen, which contains the highest concentration of Ca^{2+} within the cell. However, most of the vacuoles in the cytoplasm and nuclei of the anterior horn

neurons were empty non-membrane bound in this study, which is reminiscent of empty non-membrane-bound vacuoles observed in the cytoplasm of various cultured cells (Henics and Wheatley, 1999; Talbot and Garrett, 2001). As for vacuolar changes in the nuclei of posterior horn neurons, to a lesser extent, the involvement of posterior horn neurons is quite conceivable, judging from the presence of cholinergic interneurons, fibers and plexus in the posterior horns (Barber et al., 1984; Mesnage et al., 2011; Olave et al., 2002).

Second, vacuolar change of the nuclei of glial cells (astrocytes and oligodendrocytes) is also of great interest. Experimental disruption of non-neuronal cells such as astroglia is neurotoxic and promotes neurodegeneration (Rothstein et al., 1996). In neurodegenerative diseases, the neuron-astroglia interaction is often disrupted, as reflected by the severe loss of astroglial GLT1/EAAT2 in patients with ALS and rodent models, which causes neurotoxicity via an increase in glutamate in the extracellular space (Rothstein et al., 1992; Lauriat et al., 2007). As for the interaction between motor neurons and glial cells, analyses of chimeric mice containing a mixture of wild-type and mutant SOD1-expressing motor neurons reveal that mutant SOD1-expressing glial cells damage wild-type motor neurons, while wild-type glial cells prevent degeneration of mutant SOD1-expressing motor neurons (Clement et al., 2003). Although restricting the mutant SOD1 expression in astrocytes does not cause motor neuron degeneration (Gong et al., 2000), selective reduction of mutant SOD1 in astrocytes slows disease progression and doubles the length of disease duration after onset in mutant SOD1 transgenic mice (Yamanaka et al., 2008). In contrast, crossing neuron-specific mutant SOD1 mice with ubiquitously wild-type SOD1-expressing mice leads to wild-type SOD1 aggregation in oligodendrocytes after the onset of neuronal degeneration, and neuronal expression of mutant SOD1 is sufficient to cause motor neuron degeneration, which in turn may facilitate aggregate formation and functional deficits in surrounding glial cells (Jaarsma et al., 2008). Thus, morphological abnormality of vacuolization in the nuclei of glial cells in this study could not be directly triggered by ADAR2-knockout because of the control of ADAR2 expression by the promoter of the acetylcholine transporter gene which is selectively expressed in cholinergic neurons, but could be caused by secondary reaction of glia due to increased nuclear Ca^{2+}, judging from expression of AMPA receptors on astrocytes and oligodendrocytes (Kovács et al., 2002; Liu et al., 2002). Impairment of glial cells in turn could facilitate additional degeneration of motor neurons.

Thus, ADAR2-reduction is associated with progressive deterioration of nuclear architecture, resulting in vacuolated nuclei due to a Ca^{2+}-permeable AMPA receptor-mediated mechanism.

4. Experimental procedures

4.1. *Experimental animals*

All studies were performed in accordance with the Declaration of Helsinki, the Guidelines for Animal Studies of the University of Tokyo (Permit Number: P08-021) and the National Institutes of Health. The Committee of Animal Handling of the University of Tokyo specifically approved this study, including the experimental procedures used. All surgery was performed under sodium pentobarbital anesthesia, and all efforts were made to minimize suffering.

We used homozygous ($ADAR2^{flox/flox}$/VAChT-Cre.Fast or AR2) and heterozygous ($ADAR2^{flox/+}$/VAChT-Cre.Fast or AR2H) conditional ADAR2-knockout mice, in which the ADAR2 gene is conditionally targeted by restricted Cre expression under the control of the vesicular acetylcholine transporter gene promoter in a subset of cholinergic neurons, including the spinal motor neurons (Hideyama et al., 2010). To examine the expression level of ADAR2 that is required to edit all GluA2 mRNA or the proportion of unedited GluA2 that is not harmful to motor neurons, we studied the extent of GluA2 Q/R site editing in motor neurons lacking one ADAR2 allele in the heterozygous ADAR2 mice (Hideyama and Kwak, 2011). Because the ADAR2 gene is targeted postnatally in a manner dependent on the expression of Cre in motor neurons in AR2 mice, the time-dependent changes are illustrated by the proportion of Cre-expressing, and therefore, the proportion of ADAR2-lacking anterior horn cells in the three lines of AR2 mice in Fig.1. In AR2 and AR2H mice, Cre-mediated ablation of the ADAR2 gene occurred in a progressively larger proportion of motor neurons, and the Cre expression in AR2 mice reached the maximum level (~50% of motor neurons) by postnatal week 5 (Misawa et al., 2003). We also used homozygous $ADAR2^{flox/flox}$/VAChT-Cre.Slow (AR2Slow) mice in which the temporal profile of Cre-mediated knockout of the ADAR2 gene was slower, reaching ~50% of motor neurons by eight months of age (Hideyama and Kwak, 2011; Misawa et al., 2003). Cre expression levels were found not to differ between mice heterozygous and those homozygous for the VAChT-Cre.Fast transgene (Misawa et al., 2003). The number of ADAR2-lacking anterior horn cells significantly decreased in AR2 mice after 2 months of age as a result of Cre-dependent knock-out of ADAR2 (Hideyama et al., 2010). AR2 and AR2Slow mice displayed a slow, progressive motor dysfunction with a low rotarod performance and grip strength, the pace of which was much slower in the AR2Slow. AR2 mice showed a lower rotarod performance than did their control littermates after 5 weeks of age. Their rotarod performance rapidly declined during the initial 20–24 weeks of life, followed by stable performance until about 1.5 years of age. Grip strength declined with kinetics at about 12 weeks of age, and the decline curve was similar to that of rotarod performance. AR2 mice had long life spans, but the rate of death increased after 1.5 years of age as compared with control mice (Hideyama et al., 2010). On the other hand, heterozygous AR2H mice did not exhibit significant behavioral changes until 48 weeks of age (Hideyama and Kwak, 2011). Approximately half of ADAR2-lacking large anterior horn neurons in AR2 mice underwent degeneration between 1 and 2 months of age and the number continued to decrease thereafter beyond 1 year of age at a slower pace, while the number of ADAR2-positive anterior horn neurons remained unchanged after 2 months of age (Hideyama et al., 2010). The extent of loss of anterior horn neurons in heterozygous AR2 mice was approximately half (26%) of that observed in AR2H mice (46%) at 12 months of age (Hideyama and Kwak, 2011). Therefore, we designated the AR2H mice younger than 0.5 years of age as mice in the presymptomatic stage, AR2 mice younger than 20 weeks of age and AR2H mice younger than 1.5 years of age as mice in

early symptomatic stage, and AR2Slow mice older than 2 years of age as late symptomatic stage. We compared the differences in morphological changes of the spinal cord of the mice in these three stages as follows: we examined heterozygous AR2H mice at the age of 14 weeks and 17 weeks as representatives of presymptomatic stage, homozygous AR2 mice at the age of 15 weeks and heterozygous AR2H mice at the age of 74 weeks as representatives of early symptomatic stage and homozygous AR2Slow mice (140 weeks) as late symptomatic stage. Age-matched wild-type mice were also examined as controls. Conditional ADAR2-knockout mice and controls were examined simultaneously.

To demonstrate that the deterioration of the nuclear architecture is caused by an increased influx of Ca^{2+}, due to a low level of editing at the GluA2 Q/R site, we used AR2res ($ADAR2^{flox/flox}$/VAChT-Cre.Fast/GluR-$B^{R/R}$) mice (28 weeks and 58 weeks). In AR2res mice, the endogenous GluA2 gene (*GLIA2*) is engineered to express Q/R site-edited GluA2, rendering these mice to express normal Ca^{2+}-impermeable AMPA receptors in the absence of ADAR2 (Hideyama et al., 2010; Kask et al., 1998). Since AR2res mice do not exhibit motor dysfunction or neuronal degeneration (Hideyama et al., 2010), they are considered to be a suitable control for AR2 mice in studying the role of Ca^{2+}-permeable AMPA receptors in neuronal death-associated events including that excessive Ca^{2+}, not the failure of RNA editing at the sites other than the GluA2 Q/R site, is the cause of the large nuclear vacuoles.

4.2. *Light microscopic analysis*

The cervical levels of the spinal cord of AR2 mice (15 weeks, $n=2$), AR2Slow mice (140 weeks, $n=2$), AR2H mice (14 weeks, 17 weeks, 28 weeks, 58 weeks and 74 weeks, $n=2$, respectively), AR2res mice (28 weeks and 58 weeks, $n=1$, respectively) and control mice (14 weeks, 15 weeks, 17 weeks, 74 weeks and 135 weeks, $n=2$, respectively) were investigated. Under deep anesthesia with isoflurane, mice were transcardially perfused with 3% paraformaldehyde and 1% glutaraldehyde in PBS. The cervical cords were embedded in paraffin. Paraffin sections (5 μm thick) were stained with hematoxylin and eosin (H&E).

4.3. *Quantitative analysis of nuclear vacuoles in motor neurons*

We studied the cervical spinal cord of AR2H mice at different ages (5 weeks, 9 weeks, 17 weeks, 22 weeks, 40 weeks, 57 weeks, 61 weeks and more than 100 weeks, $n=3$–4, respectively) to count the motor neurons (mean±SEM) and the motor neurons with vacuoles (mean±SEM). Fixed spinal cord segments were cut at 10 μm with a cryotome (CM1850, Leica microsystems) after immersion with 30% sucrose PBS. Resulting sections were stained with hematoxylin, and the numbers of neurons with and without nuclear vacuoles were separately counted.

4.4. *Electron-microscopic analysis*

The cervical levels of the spinal cord of AR2 mice (15 weeks, $n=2$), AR2Slow mice (140 weeks, $n=2$), AR2H mice (14 weeks, 17 weeks, 28 weeks and 74 weeks, $n=2$, respectively), and control mice (12 weeks, 14 weeks, 15 weeks, 16 weeks, 17 weeks, 28 weeks, 74 weeks and 135 weeks, $n=2$, respectively) were investigated. Under deep anesthesia with isoflurane, mice were transcardially perfused with 3% paraformaldehyde and 1% glutaraldehyde in PBS. The spinal cords were removed and fixed in a solution (0.1 M PBS, 3.5% paraformaldehyde, 0.5% glutaraldehyde). After fixation, the spinal cords were immersed in a solution (0.2 M cacodylic acid 5 ml, 10% paraformaldehyde 2 ml, 25% glutaraldehyde 1 ml, distilled water 2 ml) for 12 h. The half anterior part at the cervical spinal cord was sectioned transversely, postfixed in 1% osmium tetroxide for several hours, dehydrated, and embedded in epoxy resin. Each block was cut into serial semi-thin sections (approximately 1 μm thick) and stained with toluidine blue. Appropriate portions of the hemi-sections of the cervical spinal cord including the anterior and posterior horns were cut into ultrathin sections, which were then stained with uranyl acetate and lead citrate for electron microscopy.

4.5. *Postmortem analysis*

The cervical and lumbar levels of the spinal cord of AR2 mice ($n=3$, 34 weeks, 30 weeks and 34 weeks, respectively) at various time courses after death including the long post mortem delay (1 h, 6 h and 24 h, respectively) were investigated at the light-and electron-microscopic levels.

Acknowledgments

This study was supported by a Grant-in-Aid for General Scientific Research (C) from the Ministry of Education, Culture, Sports, Science and Technology (22590965 to SS, 2239173 to SK) and from the Ministry of Health, Labor, and Welfare of Japan (H21-Kokoro-Ippan-017 to SK). We thank Professor Asao Hirano (Division of Neuropathology, Montefiore Medical Center, New York, NY) for his many valuable comments and suggestions.

REFERENCES

Akbarian, S., Smith, M.A., Jones, E.G., 1995. Editing for an AMPA receptor subunit RNA n prefrontal cortex and striatum in Alzheimer's disease, Huntington's disease and schizophrenia. Brain Res. 699, 297–304.

Alonso, M.T., García-Sancho, J., 2011. Nuclear $Ca2^{+}$ signaling. Cell Calcium 49, 280–289.

Andrews, J.M., Andrews, R.L., 1976. The comparative neuropathology of motor neuron disease. In: Andrews, J.N., Johnson, R.T., Brazier, M.A.B. (Eds.), Amyotrophic Lateral sclerosis: Recent research trends. Academic Press, New York, pp. 181–216.

Andrews, J.M., Maxwell, D.S., 1969. Motor neuron disease in animals. In: Norris, F.H., Kurland, L.T. (Eds.), Motor Neuron Diseases: Research on Amyotrophic Lateral Sclerosis and Related Disorders. Grune and Stratton, New York, pp. 369–385.

Barber, R.P., Phelps, P.E., Houser, C.R., Crawford, G.D., Salvaterra, P.M., Vaughn, J.E., 1984. The morphology and distribution of neurons containing choline acetyltransferase in the adult rat

spinal cord: an immunocytochemical study. J. Comp. Neurol. 229, 329–334.
Burnashev, N., Monyer, H., Seeburg, P.H., Sakmann, B., 1992. Divalent ion permeability of AMPA receptor channels is dominated by the edited form of a single subunit. Neuron 8, 189–198.
Chou, S.M., 1979. Pathognomy of intraneuronal inclusions in ALS. In: Tsubak, T., Toyokura, Y. (Eds.), Amyotrophic Lateral Sclerosis. Univ Tokyo Press, Tokyo, pp. 135–176.
Clement, A.M., Nguyen, M.D., Roberts, E.A., Garcia, M.L., Boillée, S., et al., 2003. Wild-type non-neuronal cells extend survival of SOD1 mutant motor neurons in ALS mice. Science 302, 113–117.
Corbett, A.H., Silver, P.A., 1997. Nucleocytoplasmic transport of macromolecules. Microbiol. Mol. Biol. Rev. 61, 193–211.
Dal Canto, M.C., Gurney, M.E., 1995. Neuropathological changes in two lines of mice carrying a transgene for mutant human Cu, Zn SOD, and in mice overexpressing wild-type human SOD: a model of familial amyotrophic lateral sclerosis (FALS). Brain Res. 676, 25–40.
Gong, Y.H., Parsadanian, A.S., Andreeva, A., Snider, W.D., Elliott, J.L., 2000. Restricted expression of G86R Cu/Zn superoxide dismutase in astrocytes results in astrocytosis but does not cause motoneuron degeneration. J. Neurosci. 20, 660–665.
Henics, T., Wheatley, D.N., 1999. Cytoplasmic vacuolation, adaptation and cell death: a view on new perspectives and features. Biol. Cell 91, 485–498.
Hideyama, T., Yamashita, T., Suzuki, T., Tsuji, S., Higuchi, M., Seeburg, P.H., Takahashi, R., Misawa, H., Kwak, S., 2010. Induced loss of ADAR2 engenders slow death of motor neurons from Q/R site-unedited GluR2. J. Neurosci. 30, 11917–11925.
Hideyama, T., Kwak, S., 2011. When does ALS start? ADAR2-GluA2 hypothesis for the etiology of sporadic ALS. Front. Mol. Neurosci. 4, 1–11.
Hideyama, T., Yamashita, T., Aizawa, H., Tsuji, S., Kakita, A., Takahashi, H., Kwak, S., 2012a. Profound downregulation of the RNA editing enzyme ADAR2 in ALS spinal motor neurons. Neurobiol. Dis. 45, 1121–1128.
Hideyama, T., Teramoto, S., Hachiga, K., Yamashita, T., Kwak, S., 2012b. Co-occurrence of TDP-43 mislocalization with reduced activity of an RNA editing enzyme, ADAR2, in aged mouse motor neurons. PLoS One 7, e43469.
Hirano, A., Iwata, M., 1979. Pathology of motor neurons with special reference to amyotrophic lateral sclerosis and related disease. In: Tsubak, T., Toyokura, Y. (Eds.), Amyotrophic Lateral Sclerosis. Univ Tokyo Press, Tokyo, pp. 107–132.
Jaarsma, D., Teuling, E., Haasdijk, E.D., Zeeuw, C.D., Hoogenraad, C.C., 2008. Neuron-specific expression of mutant superoxide dismutase is sufficient to induce amyotrophic lateral sclerosis in transgenic mice. J. Neurosci. 28, 2075–2088.
Kask, K., Zamanillo, D., Rozov, A., Burnashev, N., Sprengel, R., Seeburg, P.H., 1998. The AMPA receptor subunit GluR-B in its Q/R site-unedited form is not essential for brain development and function. Proc. Natl. Acad. Sci. USA 95, 13777–13782.
Kawahara, Y., Ito, K., Sun, H., Aizawa, H., Kanazawa, I., Kwak, S., 2004. Glutamate receptors: RNA editing and death of motor neurons. Nature 427, 801.
Kawahara, Y., Sun, H., Ito., K., Hideraya, T., Aoki, M., Sobue, G., Tsuji, S., Kwak, S., 2006. Underediting of GluR2 mRNA, a neuronal death inducing molecular change in sporadic ALS, does not occur in motor neurons in ALS1 or SBMA. Neurosci. Res. 54, 11–14.
Kawahara, Y., Ito, K., Sun, H., Kanazawa, I., Kwak, S., 2003. Low editing efficiency of GluR2 mRNA is associated with a low relative abundance of ADAR2 mRNA in white matter of normal human brain. Eur. J. Neurosci. 18, 23–33.
Kawahara, Y., Kwak, S., 2005. Excitotoxicity and ALS: what is unique about the AMPA receptors expressed on spinal motor neurons?. Amyotroph. Lateral Scler. 6, 131–144.
Kohn, R., 1971. Clinical and pathological findings in an unusual infantile motor neuron disease. J. Neurol. Neurosurg. Psychiat. 34, 427–431.
Kovács, A.D., Cebers, G., Cebere, A., Liljequist, S., 2002. Selective and AMPA receptor-dependent astrocyte death following prolonged blockade of glutamate reuptake in rat cerebellar cultures. Exp. Neurol. 174, 58–71.
Kwak, S., Kawahara, Y., 2005. Deficient RNA editing of GluR2 and neuronal death in amyotrophic lateral sclerosis. J. Mol. Med. 83, 110–120.
Lauriat, T.L., Richler, E., McInnes, L.A., 2007. A quantitative regional expression profile of EAAT2 known and novel splice variants reopens the question of aberrant EAAT2 splicing in disease. Neurochem. Int. 50, 271–280.
Liu, H.N., Giasson, B.I., Mushynski, W.E., Almazan, G., 2002. AMPA receptor-mediated toxicity in oligodendrocyte progenitors involves free radical generation and activation of JNK, calpain and caspase 3. J. Neurochem. 82, 398–409.
Mattson, M.P., LaFerla, F.M., Chan, S.L., Leissring, M.A., Shepel, P.N., Geiger, J.D., 2000. Calcium signaling in the ER: its role in neuronal plasticity and neurodegenerative disorders. Trends Neurosci. 23, 222–229.
Melcher, T., Maas, S., Herb, A., Sprengel, R., Seeburg, P.H., Higuchi, M., 1996. A mammalian RNA editing enzyme. Nature 379, 460–464.
Mesnage, B., Gaillard, S., Godin, A.G., Rodeau, J.L., Hammer, M., Von Engelhardt, J., Wiseman, P.W., De Koninck, Y., Schlichter, R., Cordero-Erausquin, M., 2011. Morphological and functional characterization of cholinergic interneurons in the dorsal horn of the mouse spinal cord. J. Comp. Neurol. 519, 3139–3158.
Miao, L., Schulten, K., 2009. Transport-related structures and processes of the nuclear pore complexes studies through molecular dynamics. Structure 17, 449–459.
Misawa, H., Nakata, K., Toda, K., Matsuura, J., Oda, Y., Inoue, H., Tateno, M., Takahashi, R., 2003. VAChT-Cre.Fast and VAChT-Cre.Slow: postnatal expression of Cre recombinase in somatomotor neurons with different onset. Genesis 37, 44–50.
Müller, H.A., Jeschke, R., 1971. Cytoplasmatische Vacuolen in den vorderhornganglienzellen des Menschen beim Tetanus. Virchows Arch. (Pathol. Anat.) 353, 87–98.
Olave, M.J., Puri, N., Kerr, R., Maxwell, D.J., 2002. Myelinated and unmyelinated primary afferent axons form contacts with cholinergic interneurons in the spinal dorsal horn. Exp. Brain Res. 145, 448–456.
Reif-Kohn, R., Munde, L.G., 1974. Second case of an infantile motor neuron disease. Confin. Neurol. 36, 23–32.
Rothstein, J.D., Dykes-Hoberg, M., Pardo, C.A., Bristol, L.A., Jin, L., Kuncl, R.W., Kanai, Y., Hediger, M.A., Wang, Y., Schielke, J.P., Welty, D.F., 1996. Knockout of glutamate transporters reveals a major role for astroglial transport in excitotoxicity and clearance of glutamate. Neuron 16, 675–686.
Rothstein, J.D., Martin, L.J., Kuncl, R.W., 1992. Decreased glutamate transporterby the brain and spinal cord in amyotrophic lateral sclerosis. N. Engl. J. Med. 326, 1464–1468.
Rothstein, J.D., Van Kammen, M., Levey, A.I., Martin, L.J., Kuncl, R.W., 1995. Selective loss of glial glutamate transporter GLT-1 in amyotrophic lateral sclerosis. Ann. Neurol. 38, 73–84.
Sasaki, S., Ohsawa, Y., Yamane, K., Sakuma, H., Shibata, N., Nakano, R., Kikugawa, K., Mizutani, T., Tsuji, S., Iwata, M., 1998. Familial amyotrophic lateral sclerosis with widespread vacuoles and hyaline inclusions. Neurology 51, 871–873.
Sasaki, S., Warita, H., Murakami, T., Abe, K., Iwata, M., 2004. Ultrastructural study of mitochondria in the spinal cord of transgenic mice with a G93A mutant SOD1 gene. Acta Neuropathol. 107, 461–474.
Seeburg, P.H., 2002. A-to-I editing: new and old sites, functions and speculations. Neuron 35, 17–20.

Seeburg, P.H., Single, F., Kuner, T., Higuchi, M., Sprengel, R., 2001. Genetic manipulation of key determinants of ion flow in glutamate receptor channels in the mouse. Brain Res. 907, 233–243.

Talbot, N.C., Garrett, W.M., 2001. Ultrastructure of the embryonic stem cells of the 8-day pig blastocyst before and after in vitro manipulation: development of junctional apparatus and the lethal effects of PBS mediated cell-cell dissociation. Anat. Rec. 264, 101–113.

Van Damme, P., Braeken, D., Callewaert, G., Robberecht, W., Van Den Bosch, I., 2005. GluR2 deficiency accelerates motor neuron degeneration in a mouse model of amyotrophic lateral sclerosis. J. Neuropathol. Exp. Neurol. 64, 605–612.

Yamanaka, K., Chun, S.J., Boillee, S., Fujimori-Tonou, N., Yamashita, H., Gutmann, D.H., Takahashi, R., Misawa, H., Cleveland, D.W., 2008. Astrocytes as determinants of disease progression in inherited amyotrophic lateral sclerosis. Nat. Neurosci. 11, 251–253.

Yamashita, T., Hideyama, T., Hachiga, K., Teramoto, S., Takano, J., Iwata, N., Saido, T.C., Kwak, S., 2012. A role for calpain-dependent cleavage of TDP-43 in amyotrophic lateral sclerosis pathology. Nat. Commun. 3, 1307.

Yang, J.H., Sklar, P., Axel, R., Maniatis, T., 1995. Editing of glutamate receptor subunit B pre-mRNA in vitro by site-specific deamination of adenosine. Nature 374, 77–81.

Ⅳ. ワークショップ，班会議
プログラム

厚生労働科学研究委託費　難治性疾患等克服研究事業
（難治性疾患等実用化研究事業（難治性疾患実用化研究事業））

筋萎縮性側索硬化症（ALS）新規治療法開発をめざした病態解明
平成 26 年度 ワークショップ

平成 26 年 9 月 26 日（金）10:15～15:00
都市センターホテル 601 会議室（東京都千代田区平河町 2-4-1）

10:15～　**挨　拶**

10:25～　**ALS 病態研究のフロンティア（1）**

座長：　祖父江　元（名古屋大学大学院医学系研究科　神経内科学）

1. TDP-43 のオリゴマー化・神経変性メカニズムの解明

永井　義隆（国立精神・神経医療研究センター神経研究所　疾病研究第四部）

私たちは孤発性ALSの病態解明を目指し，TDP-43の細胞質内蓄積を再現する培養細胞を用いたタイムラプスイメージング解析，およびALSモデルショウジョウバエを用いた遺伝学的解析を行った．その結果，TDP-43は微小管依存的に細胞質内を輸送され，dynactin1 の機能低下による TDP-43 の細胞質輸送低下に伴ってオリゴマー化が促進され，神経変性が増悪することが明らかになった．さらに，微小管輸送の活性化剤によりALS モデルショウジョウバエにおける TDP-43 のオリゴマー形成，神経変性が抑制されることを明らかにし，微小管輸送が ALS の治療標的になる可能性を見出した．

【Memo】

【略歴】

1990 年　大阪大学医学部　卒業
1995 年　大阪大学大学院医学系研究科　修了
1997 年　米国デューク大学神経内科・ポスドク研究員
2001 年　大阪大学大学院医学系研究科臨床遺伝学・助手
2007 年　同・准教授
2008 年　国立精神・神経センター
　　（現・(独)国立精神・神経医療研究センター）
　　神経研究所　疾病研究第四部・室長

2. ミトコンドリア浄化機構の破綻がもたらす神経変性

松田　憲之（東京都医学総合研究所）

ミトコンドリアは生体内で必須の役割を担っているが，とりわけ神経や筋肉などの非分裂細胞において重要であることが示されている．演者らは遺伝性劣性パーキンソニズムの原因遺伝子産物である PINK1 と Parkin の機能解析を手がかりにして，ミトコンドリア品質管理機構の研究を続けてきた．本講演では，ミトコンドリア浄化機能の鍵を握る「リン酸化ユビキチン」を中心に，演者らの最新の研究成果を紹介したい．

【Memo】

【略歴】

2001 年　東京大学大学院理学系研究科生物科学　卒業
　　理化学研究所・基礎科学特別研究員
　　東京都臨床医学総合研究所・外部支援研究員
　　日本学術振興会特別研究員 PD
　　理化学研究所・上級研究員　などを経て
2008 年　東京都臨床医学総合研究所・研究員
2013 年　東京都医学総合研究所・副参事研究員

11:30～　　**Hot Topics**【特別講演】

座長：　船越　洋（旭川医科大学教育研究推進センター）

■ 肝細胞増殖因子（HGF）による脊髄損傷治療の実用化研究

中村 雅也（慶應義塾大学医学部 整形外科）

我々はラット及びマーモセット脊髄損傷に対する HGF の有効性を報告してきた．その後も臨床応用に向けて，HGF の至適治療時期，最小有効濃度，髄腔内の薬理動態などの検討を継続してきた．これらの成果を結集して，平成 26 年 6 月より急性期脊髄損傷に対する第Ⅰ，□a 相治験を開始した．本治験の現状と展望に関して概説する．

【Memo】

【略歴】

1987 年　慶應義塾大学医学部 卒業
1993 年　慶應義塾大学医学部整形外科・助手
1998 年　米国ジョージタウン大学・客員研究員
2004 年　慶應義塾大学医学部整形外科・専任講師
2007 年　京都大学再生医科学研究所・非常勤講師
2012 年　慶應義塾大学医学部整形外科学・准教授
主な専門分野：　脊椎・脊髄外科，脊髄再生，iPS 細胞，神経幹細胞，神経栄養因子，Neuroimaging

12:00～昼 食 ・ 事務連絡

12:45～ **ALS 病態研究のフロンティア (2)**

座長： 阿部 康二（岡山大学大学院医歯薬学総合研究科 神経内科学）

3. 霊長類モデルを用いた TDP-43 病態の解明

大久保 卓哉、横田 隆徳（東京医科歯科大学大学院 脳神経病態学分野）

我々はカニクイザル脊髄でヒト野生型 TDP-43 を過剰発現することにより，世界初の霊長類 ALS モデルの構築に成功した．外因性 TDP-43 は注入側の前角運動神経細胞だけでなく，脊髄対側および頚髄から腰髄，大脳皮質運動野の Betz 細胞にまで拡がっていた．このモデルにおける TDP-43 の伝播機序を解明する目的で，AAV ベクターを用いてヒト野生型 TDP-43 と GFP を脊髄で同時に過剰発現させたところ，TDP-43 は GFP より広範囲に拡がっていた．TDP-43 の脊髄における伝播機序としては，局所細胞間，単一 motor column 内，異なる motor column 間の 3 つが考えられ

【Memo】

【略歴】

1998 年 東京医科歯科大学医学部医学科 卒業
2006 年 東京医科歯科大学大学院医歯学総合研究科 脳神経病態学分野 修了
同 都立墨東病院内科（神経内科）医員
2010 年 東京医科歯科大学大学院脳神経病態学・助教

4. 変異 FUS による神経変性メカニズムの解明

石垣 診祐（名古屋大学大学院医学系研究科 神経内科）

家族性 ALS/FTLD の原因遺伝子である FUS は核内で SFPQ（splicing factor, proline- and glutamine-rich）と複合体を形成するが，ALS の関連変異により SFPQ との結合は抑制され，複合体形成も阻害される．剖検脳による病理学的検討からは FUS と SFPQ の核内での共局在が家族性，孤発性 ALS/FTLD の神経細胞で低下していることがわかった．機能的に FUS と SFPQ はどちらも選択的スプライシングを通じてタウ isoform（3R/4R）のバランス変化を制御する．FUS と SFPQ の質的な機能喪失が ALS/FTLD の病態に関与する可能性が示唆された．

【Memo】

【略歴】

1996 年 名古屋大学医学部医学科 卒業
2002 年 名古屋大学大学院医学系研究科 修了
2005 年 University of Massachusetts Medical School ポスドク研究員
2010 年 名古屋大学大学院医学系研究科神経内科・特任助教

13:50～ **神経再生研究のフロンティア**

座長： 岡野 栄之（慶應義塾大学医学部 生理学教室）

5. 細胞移植による ALS 治療法開発の可能性

渡辺 保裕（鳥取大学医学部医学科脳神経医科学講座 脳神経内科学分野）

未だ有効な治療のない筋萎縮性側索硬化症（ALS）において，幹細胞を用いた移植治療は大きな注目と期待を集めている．動物実験では移植細胞の種類，移植時期，移植経路などの多様な検討が既に行われている．更に小規模ではあるが ALS 患者への細胞移植の検討が数カ国で実施されている．本講演ではこれまでの基礎的，臨床的な細胞治療の概要を紹介し，現在の細胞移植の問題と課題，今後求められる細胞治療に関して考察する．

【Memo】

【略歴】

1992 年 鳥取大学医学部医学科 卒業
1997 年 鳥取大学大学院医学系研究科 修了
同 松江赤十字病院神経内科
2000 年 鳥取大学医学部附属病院・医員
2001 年 鳥取大学医学部附属病院・助手
2003 年 グリフィス大学（オーストラリア）研究員
2004 年 鳥取大学附属病院・助手（2007 年より助教）
2010 年 鳥取大学脳神経内科・講師

6. ヒト iPS 細胞技術及び遺伝子改変動物を用いた ALS を始めとする神経変性疾患の病態の解明

岡野 栄之（慶應義塾大学医学部 生理学教室）

私たちは，ALS の新規治療法の開発を目指し，(1) iPS 細胞を用いた病態解析，(2) 霊長類を含む ALS トランスジェニックモデルの作成と解析を中心に研究を進めてきている．本ワークショップでは，これらの進捗状況について以下の点を中心として概説する．

(1) 家族性 ALS, ALS 関連疾患（SBMA, 紀伊 ALS/PDC）からの iPS 細胞の樹立と解析 ― 多検体サンプルからの効率良い iPS 細胞の樹立と神経分化誘導，表現型の迅速な解析方法の開発と孤発性 ALS を含めた今後の iPS 細胞研究の展望

(2) 家族性 ALS の原因遺伝子ヒト TDP-43 につき，これまで報告された代表的な変異を導入し，培養細胞に gene transfer を行い，最も凝集活性が強い変異型 TDP-43 遺伝子を 2 種同定．この変異型ヒト TDP-43 をマウス TDP-43 遺伝子座にノックインし，ALS モデルマウスの作成を行った．興味深いことに変異の種類により FTLD 優位型と ALS 優位型のモデルマウスが作出されるに到った．詳細な解析については，当日紹介する．尚，同じ変異を有するヒト TDP-43 を強制発現するトランスジェニックマーモセットの作成も行った．

【Memo】

【略歴】

1983 年 慶應義塾大学医学部 卒業
同 慶應義塾大学医学部生理学教室・助手
1985 年 大阪大学蛋白質研究所・助手
1989 年 Johns Hopkins 大学医学部・研究員
1991 年 東京大学医科学研究所・助手
1994 年 筑波大学基礎医学系分子神経生物学・教授
1997 年 大阪大学医学部神経機能解剖学教室・教授
2001 年 慶應義塾大学医学部生理学教室・教授
2007 年 慶應義塾大学大学院医学研究科・委員長
2008 年 Queensland Brain Institute (Australia), Honorary Professor 等 兼任

15:00～ **挨 拶**

厚生労働科学研究委託費　難治性疾患等克服研究事業
（難治性疾患等実用化研究事業（難治性疾患実用化研究事業））

筋萎縮性側索硬化症（ALS）
新規治療法開発をめざした病態解明

平成 26 年度 班会議
プログラム ・ 抄録集

平成 27 年 1 月 30 日（金）10:30～16:00

都市センターホテル 6F 601 会議室

東京都千代田区平河町 2-4-1

Tel: 03-3265-8211

1 施設　発表 **10** 分　討論 5 分

【研究代表者】　青木正志
【事務局】　東北大学大学院医学系研究科 神経内科学
〒980-8574 仙台市青葉区星陵町 1-1
TEL: 022-717-7189　FAX: 022-717-7192
E-mail: als2012@neurol.med.tohoku.ac.jp

10 min ご発表，**5** min 質疑応答

開始	終了		発表者 ・ 班員 (敬称略)	
10:30		開会のご挨拶（研究代表者）	青木 正志	
	10:40	ご挨拶（厚生労働省 疾病対策課）		
Session 1.		**遺伝子・バイオマーカー**		
		（座長）	祖父江 元	
10:40	10:55	H46R-*SOD1* 遺伝子変異を有する遺伝性ALS家系の臨床経過の解析	太田 康之	阿部 康二
10:55	11:10	孤発性ALSに認められたコピー数多型と臨床所見との関連についての検討	佐藤 秀則	加藤 丈夫
11:10	11:25	sALSではcirculating small RNAの恒常性が低下する	高橋 育子	佐々木秀直
11:25	11:40	Tg-SOD1^{G93A} の血液中変動分子の質量分析計を用いた網羅的解析	船越 洋	
Session 2.		**病態：TDP-43 と FUS**		
		（座長）	横田 隆徳	
11:45	12:00	TDP-43断片のexosomeへの選択的取り込みについて	阿部 圭輔	横田 隆徳
12:00	12:15	筋萎縮性側索硬化症運動神経細胞におけるTDP-43 mRNAの細胞内局在解析	加藤 泰介	小野寺 理
12:15	12:30	TDP-43のC末端領域の凝集に関わる配列の同定	下中 翔太郎	長谷川成人
12:30	12:45	FUSのAMPA受容体機能を介した，ALS/FTLDの症候発現	本田 大祐	祖父江 元
		昼 食 （**30**分） 班 員 会 議		
Session 3.		**その他の病態**		
		（座長）	長谷川 成人	
13:15	13:30	運動ニューロン病遺伝子*TFG* トランスジェニックマウスの作製・解析	瓦井 俊孝	梶 龍兒
13:30	13:45	オプチニューリンノックアウトマウスの作製と評価	倉持 真人	川上 秀史
13:45	14:00	Cystatin C による運動神経保護メカニズムの解明	渡邊 征爾	山中 宏二
14:00	14:15	神経変性を防止する膜電位依存的ミトコンドリア品質管理機構	松田 憲之	田中 啓二
		休 憩（**15**分）		
Session 4.		**再生 ・ iPS細胞 ・ 治療法開発**		
		（座長）	郭 伸	
14:30	14:45	ALSラットモデル微小血管周皮細胞の新生	割田 仁	青木 正志
14:45	15:00	iPS細胞と遺伝子改変動物を用いたALSの病態研究	岡野 栄之	
15:00	15:15	ES/iPS細胞からの運動ニューロン分化を促進する低分子同定のための化合物ライブラリースクリーニング	後藤 和也	髙橋 良輔
15:15	15:30	2-DGを用いたALSの戦略的治療	加藤 信介	
15:30	15:45	モデル動物を用いた孤発性ALSの治療法開発研究	郭 伸	
15:50		閉会のご挨拶（研究代表者）	青木 正志	

Ⅴ．班体制

班体制

筋萎縮性側索硬化症（ALS）新規治療法開発をめざした病態解明

区　分	氏　名	所　属　等	職名
研究代表者	青木 正志	東北大学大学院医学系研究科神経内科学	教　授
研究分担者 （五十音順）	浅田 隆太	名古屋医療センター臨床研究センター臨床研究事業部研究開発推進室	室　長
	阿部 康二	岡山大学大学院医歯薬学総合研究科神経内科学	教　授
	岡野 栄之	慶應義塾大学医学部生理学	教　授
	小野寺 理	新潟大学脳研究所分子神経疾患資源解析学分野	教　授
	郭　伸	東京大学大学院医学系研究科附属疾患生命工学センター臨床医工学部門	客員研究員
	梶　龍兒	徳島大学大学院ヘルスバイオサイエンス研究部臨床神経科学分野	教　授
	加藤 信介	鳥取大学医学部病理学講座脳病態医科学分野	准教授
	加藤 丈夫	山形大学医学部器官病態統御学生命情報内科学分野	教　授
	川上 秀史	広島大学原爆放射線医科学研究所分子疫学研究分野	教　授
	佐々木秀直	北海道大学大学院医学研究科神経内科学分野	教　授
	祖父江 元	名古屋大学大学院医学系研究科神経内科学	教　授
	高橋 良輔	京都大学大学院医学研究科臨床神経学	教　授
	田中 啓二	東京都医学総合研究所	所　長
	長谷川成人	東京都医学総合研究所認知症・高次脳機能研究分野	分野長
	船越　洋	旭川医科大学教育研究推進センター	教授・センター長
	山中 宏二	名古屋大学環境医学研究所病態神経科学分野	教　授
	横田 隆徳	東京医科歯科大学大学院医歯学総合研究科脳神経病態学	教　授
事務局	割田　仁	東北大学大学院医学系研究科神経内科学	